BEHAVIOUR OF SHORT FATIGUE CRACKS IN A NAVAL STEEL

A. El Malki Alaoui*, D. Thevenet*, A. Zeghloul**
*Mechanics of Naval and Offshore Structures Laboratory **LPMM
*2 rue François Verny, F-29806 Brest Cedex 9 **Ile du Saulcy, F-57045 Metz Cedex 1
malkiaab@ensieta.fr, thevenda@ensieta.fr, zeghloul@lpmm.univ-metz.fr

Introduction

Fatigue damage in a steel (S355NL type) employed in ship structures was investigated. Damage starts with initiation of one or more cracks around a defect or an inhomogeneity producing a local stress concentration [1, 2]. These cracks propagate creating local plastic strain in an overall elastic material: the structure cracks in elasto-plastic mode [3, 4]. The damage tolerance concept is now largely used to evaluate fatigue life of structures and current fracture mechanics methods for fatigue assessment are generally based on long crack behaviour, including those that consider thresholds for crack propagation.

The purpose of this study is to analyse short fatigue cracks initiation and propagation and examine differences between short and long cracks taking into account loading conditions and closing effects. Before exposing short and long cracks results, a description of experimental procedure will be done.

EXPERIMENTAL PROCEDURE

In order to characterise fatigue cracks behaviour, tests were carried out in laboratory air and at room temperature (20°C) with constant stress ratio from 0.1 to 0.5. Tests were performed on a hydraulic machine with capacity of 100 kN. In this work, two kinds of samples were used in order to study long crack and short crack propagation. Initially, a conventional sample (SEN type) containing a short slot was used to determine the “reference” behaviour corresponding to the long crack propagation rate: da/dN versus ΔK_{eff}. This short slot (4 mm in length) was performed by electro-discharged machining (EDM) using a 290 µm diameter wire. Then, a block specimen was chosen to examine the short crack propagation rate. In order to locate the crack initiation site and make easier observation and measurements, a large circular notch (20 mm in radius) was machined. For these specimens, no pre-cracking was performed and cracks appear naturally. A finite element calculation allowed to determine the maximum stress value in elastic case. The notch stress concentration factor (SCF) is about 1.92.

First of all, tests using the decreasing ΔK method were performed on the conventional sample (SEN) in order to determine the stress intensity factor threshold ΔK_{th}. The load range was gradually decreased until no further crack growth was observed. At this stage, a ΔK_{th} value was calculated. Before decreasing load, we ensured that crack left its induced plastic zone created by the previous loading. During crack propagation, lips remain in contact even when the load applied is no null [5]. In order to obtain experimentally fatigue crack opening load, the compliance method was used by sticking a strain gauge in back of the specimen to measure

ligament strain of the specimen. Indeed, in proportion as the crack advances, the crack closure effect occurs and then load-strain curve lets appear a slope change. For instance, Fig. 1 represents load versus ligament strain (P, δ).The opening load P_{op} determined from these curves is that for which crack is completely opened. Throughout the tests, opening load P_{op}, needed in calculation of the effective stress intensity factor range ΔK_{eff}, was measured: $K_{eff} = K_{max} - K_{op}$.

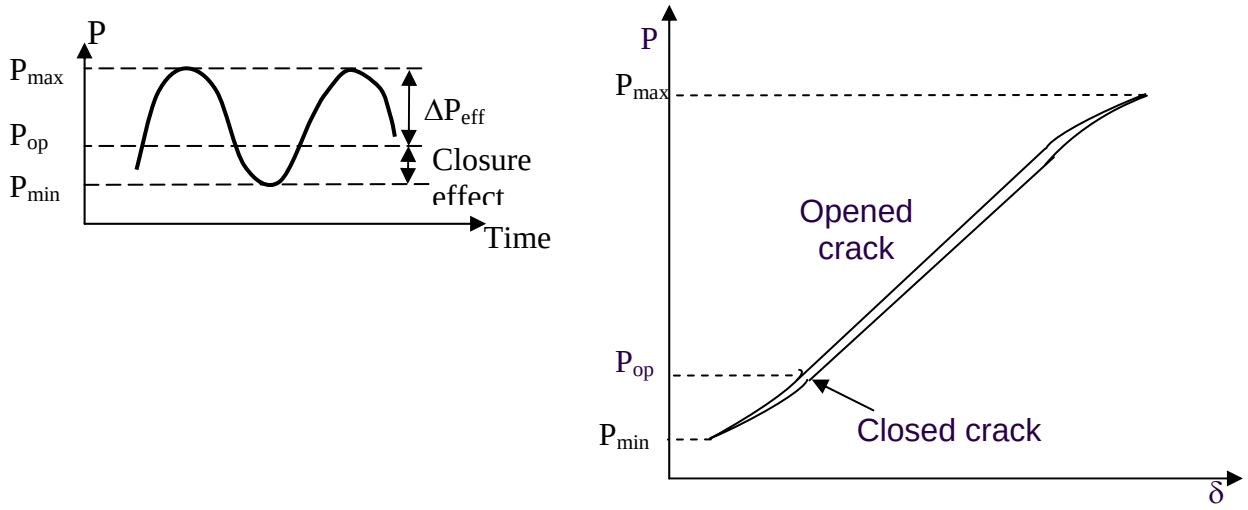

FIGURE 1. Schematic diagrams of load vs. ligament strain induced by the load range above and below the opening load

With a view to improve optical measurements of the crack advance, each specimen was mechanically polished using Si-C papers and diamond pastes (9, 3 and 1 μm).

Two methods were selected to detect and follow fatigue cracks initiation and propagation on the specimen surface: plastic replica and far-field microscope. These techniques are very useful when the crack initiation site is not known, in particular in the short cracks cases. The plastic replica method consists in applying an “cellulose acetate” sheet dissolved in acetone on specimen surface and recovering plastic film. In order to obtain replicas, fatigue tests were periodically stopped each 5000-10000 cycles, according to the applied loading amplitude and specimen fatigue life. The far-field microscope technique (coupling with a CCD camera) uses a strong magnification to follow crack propagation from notch and allow to take photos at each regular stops until fracture. Plastic replica and pictures were taken at mean stress level. After fracture, plastic replicas were observed under optical microscope or pictures what makes it possible to go up the crack history leading to fracture and other non propagative cracks (Fig. 2). All tests were conducted at room temperature (20°C), frequency 35 Hz and using a sinusoidal waveform with constant load ratio R from 0.1 to 0.5.

Finally, analyses concerning cracked surfaces were carried out using an optical microscope and a scanning electron microscope (SEM).

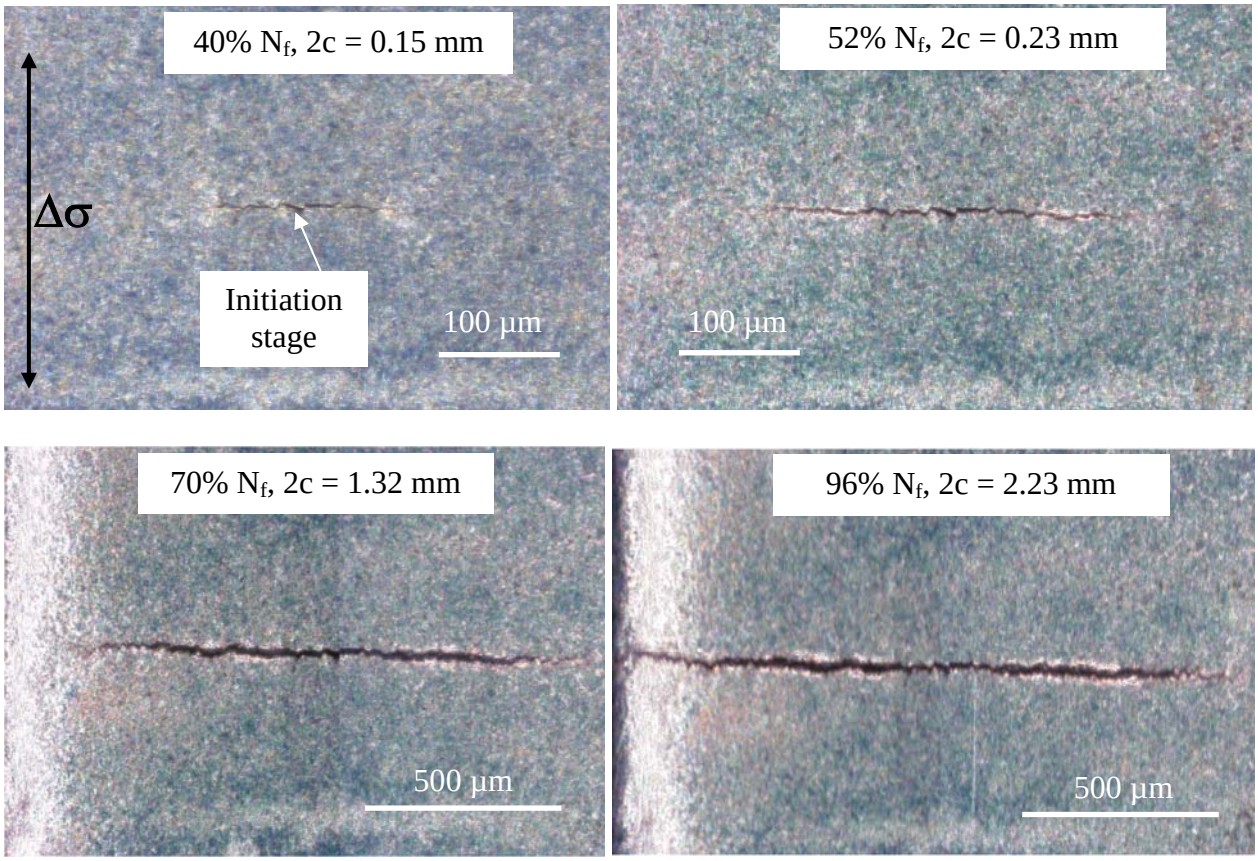

FIGURE 2. Pictures set corresponding to the main crack (R = 0.5)

Results and discussions

For S355NL steel, long fatigue cracks (LC) results are given on Fig. 3 for stress ratios R = 0.1 and 0.5. Especially, these results show crack propagation rate versus stress intensity factor range $\Delta K = K_{max} - K_{min} = K_{max}(1-R)$. Propagation rate was calculated from couples (a, N) measured during tests. Indeed, the well-known method of sequences [6] was used, what allowed to evaluate $(da/dN - \Delta K)$ using two adjacent couples (a_{i-1}, N_{i-1}) and (a_i, N_i):

$$\frac{da}{dN} = \frac{a_i - a_{i-1}}{N_i - N_{i-1}}$$

Stress intensity factor values K have been evaluated from polynomial formulas. These formulas are given by [7]:

$$K = K_0\left[1.99\left(\frac{a}{w}\right)^{1/2} - 0.41\left(\frac{a}{w}\right)^{3/2} + 18.7\left(\frac{a}{w}\right)^{5/2} - 38.48\left(\frac{a}{w}\right)^{7/2} + 53.85\left(\frac{a}{w}\right)^{9/2}\right]$$

Where

$$K_0 = \frac{P}{e\sqrt{w}}$$

With P applied load, e specimen thickness, W ligament length and a crack length.

On Fig. 3, it clearly appears that propagation rate depends on the stress ratio R. These results confirm there is a long crack threshold ΔK_{th} for each load ratio. For this steel, long cracks thresholds are about 6.4 MPa.m$^{1/2}$ and 5.4 MPa.m$^{1/2}$ respectively for R = 0.1 and 0.5. This difference can be explained by crack closure effects. Values evaluated by the compliance method (Fig. 1) allowed to plot the "reference behaviour" corresponding to the long crack propagation rate : da/dN versus ΔK_{eff}. Only one threshold $\Delta K_{eff,th}$ = 4.7 MPa.m$^{1/2}$ still exists when da/dN versus ΔK_{eff} is plotting. These results show that propagation rate does not present any dependence on stress ratio when they are represented from ΔK_{eff} [8].

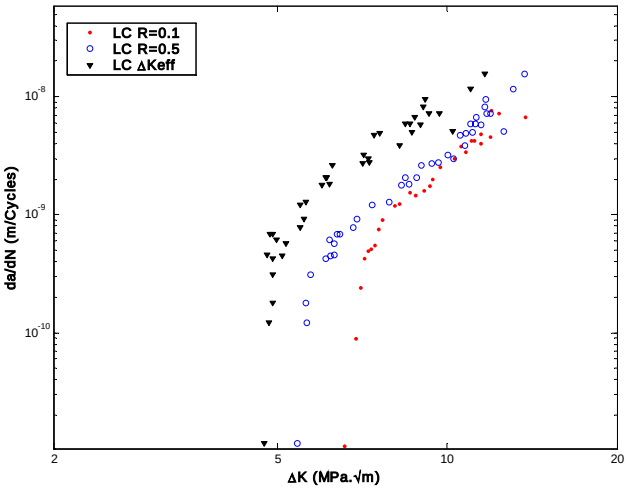

FIGURE 3. Stress ratio effect on the fatigue crack growth in S355NL steel.

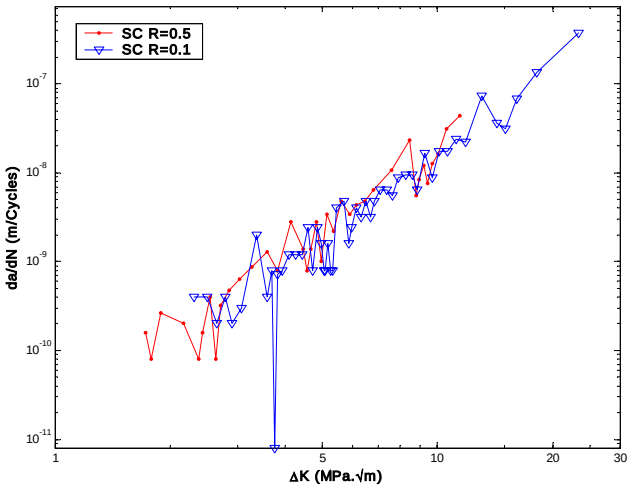

FIGURE 4. Propagation rate da/dN versus ΔK for small cracks in S355NL steel.

The main topic of the present work was to characterise the short crack (SC) behaviour in S355NL steel. This was achieved by comparing short cracks results with long cracks ones obtained previously. In order to establish these two behaviours, the loading conditions employed for long cracks tests were applied to short cracks tests. In each case, in order to ensure the reproducibility of the phenomenon, several tests were performed. Short cracks results, issued from tests conducted at R = 0.1 and 0.5, are represented on Fig. 4. In order to visualise various cracks accelerations and decelerations, points were connected by lines. In all cases, stress intensity factor K was calculated by FEM by using Abaqus Standard V6.3. Results were compared to the Newman and Raju relations [9] and seemed to be in good agreement. Similarities could be observed concerning propagation rate for these two load ratios. In fact, two

parts can be distinguished in this curve. In the R = 0.1 case and for ΔK values lower than 4.0 MPa.m$^{1/2}$ (2.5 MPa.m$^{1/2}$ for R = 0.5), decelerations appear until a temporary crack arrest (da/dN ≈ 0). In all cases, significant decelerations of the propagative crack were also noted: a rate gap appears in Fig. 4. For higher ΔK values, rate becomes more regular and increases with increasing ΔK until fracture.

Crack length (a) versus number of cycles (N) is represented on Fig. 5 for load ratio R = 0.3. This curve shows that cracks progressively propagated until a crack length for which they are blocked during several thousands of cycles or they definitively stopped (non propagative crack). Typically, the number of cracks increases during tests but only one crack tends to become a propagative fatigue crack and propagation of all other cracks stops.

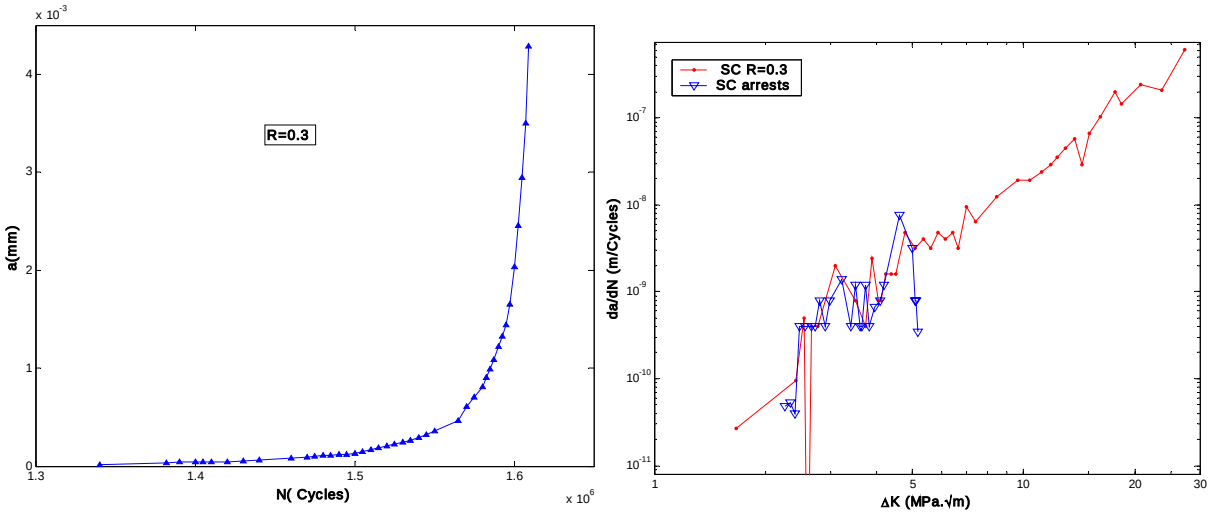

FIGURE 5. Fatigue crack growth and da/dN versus ΔK (R = 0.3). Propagative and non propagative cracks.

In order to compare short and long cracks behaviour through a crack closure criterion, short and long crack propagation data were plotted using ΔK_{eff} values calculated by relation: $\Delta K_{eff} = K_{max} - K_{op}$ for R = 0.1 (Fig. 6).

First of all, for a given ΔK, small cracks propagated faster than long cracks. In Fig. 6, it can be noticed that for crack length (a) lower than 400 µm, all small cracks propagated for ΔK lower than the threshold value $\Delta K_{eff,th}$, moreover small crack propagation rate decreases until a minimum before going up again gradually with ΔK increasing. Short cracks propagated quickly and irregularly before joining long crack behaviour. So, present results are enough closed to predict no crack closure effect concerning short cracks. Nevertheless, measurements inaccuracy does not permit to conclude definitively [10].

Using ΔK_{eff} to present long cracks results allowed to ensure a real comparison between long and short crack propagation behaviours: using ΔK_{eff} displaces da/dN curves towards left and reduces differences between short and long cracks propagation rate. This study shows short fatigue cracks in S355NL steel do not present a growth threshold. However, it does not a similarity in the area under threshold for long and short cracks, since the short cracks still start

and propagated with an accelerated or decelerated rate for ΔK below long cracks ΔK_{th} values. The same observations are valid for load ratio R = 0.3 as R = 0.5. For several load ratios, differences between short and long cracks behaviours decrease when ΔK value is increasing. Meeting of these two curves is done from a ΔK about 6.5 MPa.$m^{1/2}$, that is to say a crack length about 400 µm.

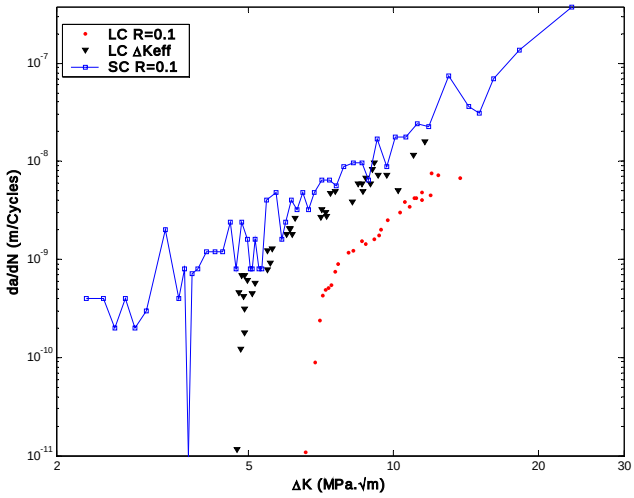

FIGURE 6: Comparison between fatigue crack growth for small and long cracks.

After fracture, several cracks let appear a significant “yawning” (Fig. 7). Inside the sample, fatigue cracks not always propagated perpendicularly to the loading direction, but could present deviations at microscopic level leading to a mixed mode propagation: opening mode and shearing mode. The superposition of these effects could explain the “yawning” observed in Fig. 7.

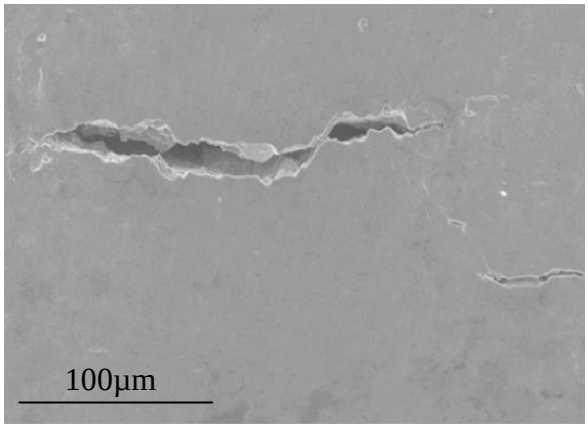

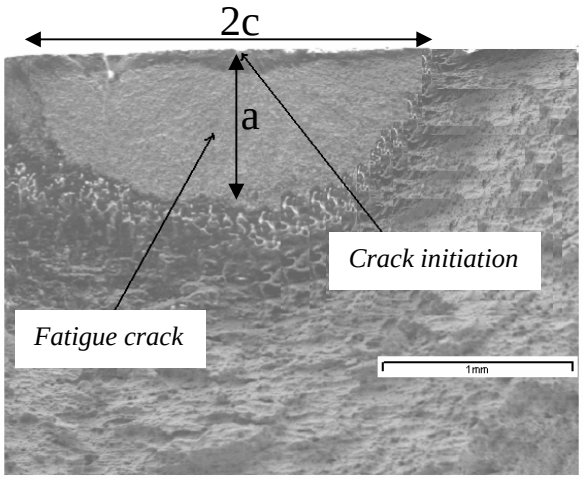

FIGURE 7. Surface crack (yawning)
FIGURE 8. Crack shape (MEB)

In order to observe various damages around crack and its profile geometry, we carried out crack shape analysis. This analysis showed a semi-elliptical crack profile on the cracked surface and the ratio between crack depth (a) and crack length (2c) was measured: $a/2c \approx 0.4$ (Fig. 8). This ratio then makes it possible to calculate stress intensity factor ΔK for a semi-elliptic crack shape, by using Abaqus Standard V6.3 and according to the Newman and Raju expressions [9].

Conclusion

Short cracks propagated quickly and irregularly for $\Delta K < \Delta K_{eff,th}$, with important rate variations. Propagation rate variations are often associated to interactions between cracks and grain boundaries or other microstructural barriers, crack deviations and change in propagation mode [11-13]. In case of multiple cracking, cracks interact between each other: this can influence their propagation rate and lead to a deceleration or even a crack arrest [14]. This behaviour observed for short cracks is also due to a important crack closure effect for long cracks at the threshold level. Indeed, micrographies showing cracking ways indicate that they are more tortuous with branching.

Finally we can summarize process of appearance for a macroscopic crack in specimen:

- After a number of cycles, modifications of mechanical characteristics can be observed and microscopic cracks appeared with a increasing number, until a comparable dimension with microstructural barriers, then,
- Propagation of one crack or coalescence of several cracks, and finally,
- A main crack appears and propagates until fracture.

References

1. Newman, J.C. et al, Fatigue-life prediction methodology using small-crack theory, *Int. J. Fatigue*, **2**, 109-119, 1999.
2. Blochwitz, C., Richter, R., Plastic strain amplitude dependent surface path of microstructurally short fatigue cracks in face-centred cubic metals. *Materials Science and Engineering, A267*, 120-129, 1999.
3. Bathias, C., Baïlon, J.P., *La fatigue des matériaux et des structures*, Editions Hermes, 1997.
4. Zeghloul, A., *Comparaison de la propagation en fatigue des fissures courtes et des fissures longues*, Doctorat d'état en Sciences Physiques, 1988.
5. Elbert, W., *ASTM STP 486*, American Society for Testing and Materials, 230-242, 1971.
6. Lieurade, H.P., *La pratique des essais de fatigue*, PYC Edition Paris 1982.
7. Rooke, D.P., Cartwright, D.J. *Compendium of stress intensity factors*, London HMSO, 1975.
8. Lawson, L. et al. Microstructural fracture in metal fatigue. *Int. J. Fatigue,* **19**, Supp. No. 1, S61-S67, 1997.
9. Newman, J.C., Raju I.S. Stress Intensity Factor Equations for Cracks in Three-dimensional Finite Bodies, *Fracture Mechanics: Fourteenth Symposium Volume I : Theory and Analysis, ASTM STP 791,* J.C. Lewis and G. Sines, Eds., American Society for Testing and Materials, pp. I-238I-265, 1983.

10. Chan K.S. et al, Fatigue crack growth mechanisms in HSLA-80 steels, *Materials Science and Engineering, A222*, 1-8, 1997.

11. Kaynak, C. A. Ankara and T.J. Baker, A comparison on short and long fatigue crack growth in steel, *Int. J. Fatigue*, **18**, No 1, 17-23, 1996.

12. Chapetti, M.D. et al. Two small-crack extension force concept applied to fatigue limit of blunt notched components, *Int. J. Fatigue*, **21** 77–82, 1999.

13. Grabowski, L. and King, J. F.. Modelling short crack behaviour in nickel-base superalloys, *Fatigue Fract. Engng Mater.Struct.***15**, 6, 595-606, 1992.

14. Jiang, Z.D. J.Petit and G.Bezine, Stress intensity factors of two parallel 3D surface crack, *Eng. Fract. Mech.*, **40**, N°2 pp 345-354, 1991.